GAUSSIAN BLUR ESTIMATION FOR PHOTON-LIMITED IMAGES

Jizhou Li[1], *Feng Xue*[2] *and Thierry Blu*[1]

[1] Department of Electronic Engineering, The Chinese University of Hong Kong, Hong Kong
[2] National Key Laboratory of Science and Technology on Test Physics and Numerical Mathematics, Beijing, China

ABSTRACT

Blur estimation is critical to blind image deconvolution. In this work, by taking Gaussian kernel as an example, we propose an approach to estimate the blur size for photon-limited images. This estimation is based on the minimization of a novel criterion, blur-PURE (Poisson unbiased risk estimate), which makes use of the Poisson noise statistics of the measurement. Experimental results demonstrate the effectiveness of the proposed method in various scenarios. This approach can be then plugged into our recent PURE-LET deconvolution algorithm, and an example on real fluorescence microscopy is presented.

Index Terms— Parametric blur estimation, Poisson noise, photon-limited images, image deconvolution.

1. INTRODUCTION

Images acquired under photon-limited conditions are fundamentally limited in resolution by diffraction and corrupted by Poisson noise. This degradation happens in many applications such as fluorescence microscopy or astronomy, due to various physical constraints (e.g. low-power light source, short exposure time). Image deconvolution is an effective tool to improve the quality of the measured images [1–4]. When the imaging point-spread function (PSF) of the optical system is unknown, a single blurred and noisy image is the only input. In that case, we need to estimate both the original image and the PSF. Thus current high-quality non-blind deconvolution algorithms [5–9] cannot be used directly.

A number of techniques have been proposed to address this problem. One popular approach consists in estimating simultaneously both the original image and the PSF, based on *prior* hypotheses on the original image and the blur kernel [1, 10, 11]. Alternatively, we can also first identify the PSF, and then carry out non-blind deconvolution to obtain the restored image. Indeed, the knowledge of the imaging system often suggests a parametric form for the PSF. For example, the PSF of 3D wide-field fluorescence microscopy is often assumed to be the Gibson-Lanni model [12–14]. In 2D confocal microscopy, the PSF can be well approximated by a Gaussian function dependent on its variance [15, 16]. In this context, during the restoration process, only a small number of parameters of the PSF need to be estimated, thus dramatically reducing the number of degrees of freedom in the blur estimation problem [17–19]. Parametric blur estimation has been applied in linear motion blur [20], atmospheric turbulence [21], astronomical imaging [22, 23] and fluorescence microscopy [16, 24].

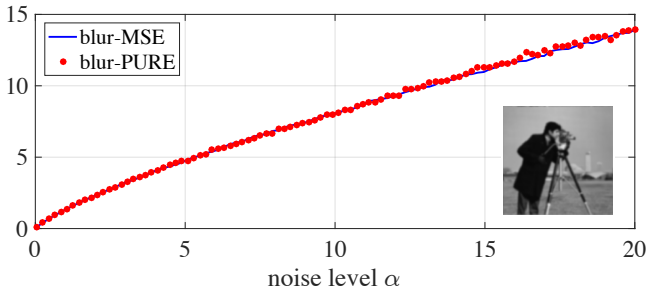

Fig. 1. Close match between the *blur-MSE* and the blur-PURE under a wide range of noise levels. The maximum difference is 0.59. Example: *Cameraman* image (256×256) degraded by Gaussian kernel ($s_0 = 2.0$) and Poisson noise ($\alpha \in [0.05, 20]$).

Typical parametric PSF models include Gaussian kernel [19, 25, 26], out-of-focus blur [27, 28], motion blur [20] and *anisotropic* Gaussian function [19]. Li *et al.* [21] proposed to estimate the turbulence blur parameter via kurtosis minimization. Carasso [23] identified the blur size by fitting the Gaussian kernel to the observed image, utilizing the property of the fast Fourier decrease of the Gaussian kernel. Chen and Ma [26] chose the Gaussian blur parameter based on the maximization of the differential coefficients of restored image Laplacian ℓ_1-norm curve. In the work of [29], generalized cross validation (GCV) is validated to determine the parameters of motion blur and out-of-focus blur. We previously proposed a criterion based on Stein's unbiased risk estimate (SURE) for the estimation of several types of PSF [19].

These approaches, however, become sub-optimal for photon-limited images due to the signal-dependent nature

This work was supported by grants from the Research Grants Council of Hong Kong (AoE/M-05/12, CUHK14200114), and in part by the National Natural Science Foundation of China (61401013).

of Poisson noise (see Section 4). In this work, we extend the blur-SURE criterion introduced in [19] to the Poisson noise case. It is based on the Poisson unbiased risk estimate (PURE) [9, 30] and named as blur-PURE. The parameters of the PSF are then chosen in such a way as to minimize this new objective functional over a family of Wiener processings. We exemplify this strategy using a Gaussian PSF since it can be used in many real applications [15, 16, 26]. The blur size is then the only parameter to be identified. Once the PSF is retrieved, our recent non-blind deconvolution algorithm [9] is carried out.

The paper is organized as follows: Section 2 introduces the theoretical basis of this work, specifically the proposed blur-PURE criterion; in Section 3, we exemplify this criterion with Gaussian blur estimation; finally we present experimental results that illustrate the effectiveness of the proposed approach.

2. THEORETICAL BACKGROUND

2.1. Problem statement

For photon-limited images, the observation model caused by blurring and Poisson noise is given by

$$\mathrm{y} = \alpha\, \mathcal{P}\left(\frac{\mathbf{H}_0 \mathrm{x}}{\alpha}\right) \tag{1}$$

where $\mathrm{y} \in \mathbb{R}^N$ denotes the distorted observation of the unknown true image $\mathrm{x} \in \mathbb{R}_+^N$, $\mathbf{H}_0 : \mathbb{R}^N \to \mathbb{R}^N$ implements a convolution of the PSF h, which is unknown as well. $\mathcal{P}(\cdot)$ represents the effect of Poisson noise[1] and $\alpha \in \mathbb{R}_+$ is the amplification factor, which controls the strength of noise. Specifically, larger values of α will lead to higher Poisson noise. We estimate its value using a robust linear regression performed on a collection of local estimates of the sample mean and sample variance, similar to [30] and [31].

The objective of this work is to obtain an estimate $\mathbf{H}$ of the ground truth $\mathbf{H}_0$. It can be shown, using standard Wiener theory arguments, that the best linear processing $\mathbf{U}$ that minimizes the expected mean squared error (MSE) $\frac{1}{N}\mathcal{E}\{\|\mathbf{U}\mathrm{y} - \mathbf{H}_0\mathrm{x}\|^2\}$ is of the form

$$\mathbf{U}_{\mathbf{H}_0,\lambda_0} = \mathbf{H}_0\mathbf{H}_0^{\mathrm{T}}\left(\mathbf{H}_0\mathbf{H}_0^{\mathrm{T}} + \lambda_0 \mathbf{S}_{\mathrm{x}}^{-1}\right)^{-1},$$

where $\mathbf{S}_{\mathrm{x}} = \mathcal{E}\{\mathrm{x}\mathrm{x}^{\mathrm{T}}\}$ is the covariance matrix of x (assumed to be stationary) and λ_0 is some constant (depends on the noise level α and the mean value of x). This oracle criterion is named as *blur-MSE*. Note that since $\mathbf{H}_0$ is a convolution matrix, $\mathbf{U}_{\mathbf{H}_0,\lambda_0}$ can be directly implemented in the Fourier domain as:

$$\mathbf{U}_{\mathbf{H}_0,\lambda_0}(\omega) \overset{\text{Fourier}}{\rightsquigarrow} \frac{|H_0(\omega)|^2}{|H_0(\omega)|^2 + \frac{\lambda_0}{\mathbf{S}_{\mathrm{x}}(\omega)}},$$

[1] $\mathcal{P}(\mathrm{z})$ is a Poisson random variable of mean z, iff the probability of $\mathcal{P}(\mathrm{z}) = \mathrm{m} \in \mathbb{R}_+^N$ is $\prod_{i=1}^N \frac{z_i^{m_i} e^{-z_i}}{m_i!}$.

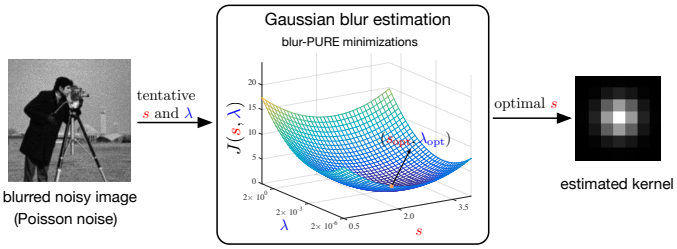

Fig. 2. Flow chart of the proposed approach for Gaussian blur estimation. The regularization parameter λ and blur parameter s (corresponding to $\mathbf{H}$) are estimated jointly, by minimizing $J(s, \lambda)$ defined in (5). Once the blur kernel is available, a non-blind deconvolution algorithm [9] can be applied to obtain the restored image.

where $\omega = (\omega_1, \omega_2)$ is the (zero-centered) 2D DFT frequency variables and $\|\omega\|^2 = \omega_1^2 + \omega_2^2$, $H_0(\omega)$ is the Fourier representation of $\mathbf{H}_0$.

In this work, since $\mathbf{S}_{\mathrm{x}}$ is unknown, we approximate $\mathbf{S}_{\mathrm{x}}^{-1}$ as $\mathbf{P}^{\mathrm{T}}\mathbf{P}$ where $\mathbf{P}$ is the discrete Laplacian operator ($\|\omega\|^2$). Our strategy consists in minimizing

$$\text{blur-MSE} = \frac{1}{N}\mathcal{E}\{\|\mathbf{U}_{\mathbf{H},\lambda}\mathrm{y} - \mathbf{H}_0\mathrm{x}\|^2\}, \tag{2}$$

over $\mathbf{H}$ and λ, where

$$\mathbf{U}_{\mathbf{H},\lambda} = \mathbf{H}\mathbf{H}^{\mathrm{T}}\left(\mathbf{H}\mathbf{H}^{\mathrm{T}} + \lambda \mathbf{P}^{\mathrm{T}}\mathbf{P}\right)^{-1}. \tag{3}$$

Similar to [19], it can be shown that for all $\mathbf{W}_{\mathbf{H}}$, the solution $\mathbf{H}$ of (2) that minimizes the blur-MSE is related to the true matrix $\mathbf{H}_0$, say $\mathbf{H}\mathbf{H}^{\mathrm{T}} = \mathbf{H}_0\mathbf{H}_0^{\mathrm{T}}$.

However, in practice we cannot minimize the *blur-MSE* directly since $\mathbf{H}_0\mathrm{x}$ is unknown. Instead, we will use an unbiased estimate of its expected value, blur-PURE, for the minimization. It solely depends on the observed image y thus is computable.

2.2. Blur-PURE for linear processing

For the linear degradation model (1), we have the following theorem.

Theorem 1 *Consider the Poisson degradation model* (1) *and* $\mathbf{U}$ *an arbitrary matrix, the random variable*

$$\begin{aligned}\text{blur-PURE} = \frac{1}{N}||\mathbf{U}\mathrm{y}||^2 + \frac{1}{N}\|\mathrm{y}\|^2 - \frac{\alpha}{N}\mathbf{1}^{\mathrm{T}}\mathrm{y} \\ - \frac{2}{N}\sum_{n=1}^{N} \mathrm{y}^{\mathrm{T}}\mathbf{U}(\mathrm{y} - \alpha\, \mathrm{e}_n),\end{aligned} \tag{4}$$

is an unbiased estimate of the blur-MSE; i.e.,

$$\mathcal{E}\{\text{blur-PURE}\} = \frac{1}{N}\,\mathcal{E}\left\{||\mathbf{U}\mathrm{y} - \mathbf{H}_0\mathrm{x}||^2\right\},$$

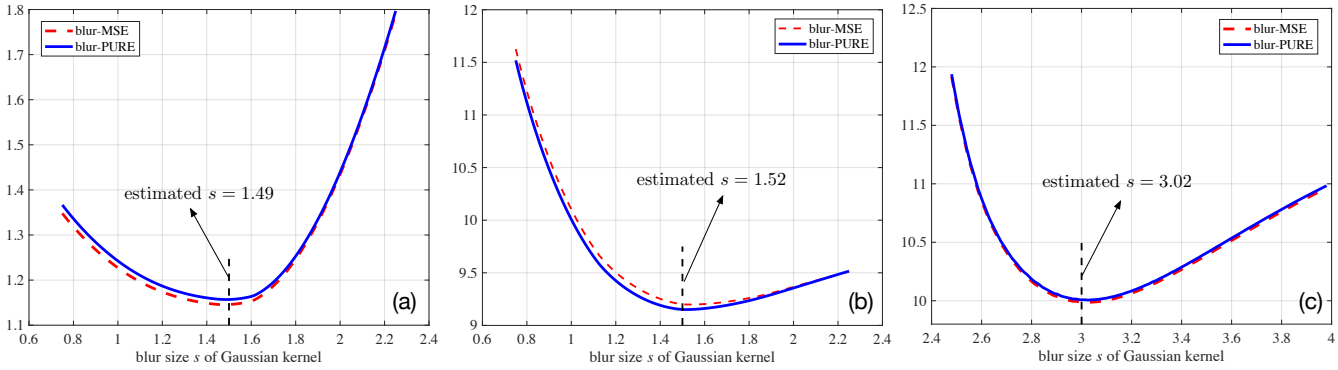

Fig. 3. Typical examples of the *blur-MSE* and blur-PURE minimizations. Images are degraded by Gaussian kernel (ground truth blur size s_0) and Poisson noise (amplification factor α). (a) *Cameraman* image ($s_0 = 1.5$, $\alpha = 1$); (b) *Cameraman* image ($s_0 = 1.5, \alpha = 10$); (c) *Lake* image ($s_0 = 3.0, \alpha = 10$). All of them can obtain highly accurate estimate of the blur size by minimizing the blur-PURE (also the *blur-MSE*).

where e_n *is the* N*-dimensional vector with components* $\delta_{k-n}, k = 1, 2, ..., N$*, and* N *is the pixel number of the image.*

The unbiasedness between blur-PURE and *blur-MSE* and the fact that the pixel number of the image N is large (typically, $256 \times 256 = 65536$) indicate that (4) can be used as a reliable subsitute of the *blur-MSE* (law of large numbers). Thus by using the approximation $\mathbf{U}_{\mathbf{H},\lambda}$ in (3) and minimizing (4), the optimal $\mathbf{H}$ and λ can be obtained in practice. Fig. 1 shows a typical example showing the blur-PURE matches the *blur-MSE* under a wide range of noise levels, indicating the blur-PURE is a reliable estimator of the *blur-MSE*.

3. BLUR-PURE BASED GAUSSIAN BLUR ESTIMATION

By taking Gaussian kernel as an example, in this section we exemplify the blur-PURE criterion for the blur estimation. We denote the ground truth parameter by s_0. The Gaussian kernel is characterized by

$$\mathbf{h}_s(i, j; s) = C \cdot \exp(-\frac{i^2 + j^2}{2s^2})$$

with variance s^2, where (i, j) denotes the 2D coordinates, C is a normalization coefficient and s is the unknown blur size to be estimated.

Consequently, the estimation of the true s_0 and optimal λ_0 can be formulated as the following minimization problem:

$$(s_0, \lambda_0) = \underset{s,\lambda}{\operatorname{argmin}} J(s, \lambda),$$

where

$$J(s, \lambda) = \frac{1}{N}||\mathbf{U}_{\mathbf{H}_s,\lambda}\mathrm{y}||^2 + \frac{1}{N}\|\mathrm{y}\|^2 - \frac{\alpha}{N}\mathbf{1}^{\mathrm{T}}\mathrm{y} - \frac{2}{N}\sum_{n=1}^{N}\mathrm{y}^{\mathrm{T}}\mathbf{U}_{\mathbf{H}_s,\lambda}(\mathrm{y} - \alpha\,\mathrm{e}_n). \quad (5)$$

In order to determine these two scalar variables (s and λ), we perform a simple exhaustive search over all the possible values in a certain range [19]. The procedure is as follows: for each fixed s, the corresponding optimal λ is determined by $\lambda_0(s) = \underset{\lambda}{\operatorname{argmin}} J(s, \lambda)$; then the function $\lambda_0(s)$ will be used to find the optimal s by solving $s_0 = \underset{s}{\operatorname{argmin}} J(s, \lambda_0(s))$. For a 256×256 image, if we use 30 discrete candidate points for s and λ, the exhaustive search requires $30 \times 30 = 900$ computations of the blur-PURE. The proposed approach is summarized in Fig. 2. For the case of multiple blur parameters to be estimated, more sophisticated minimization algorithms such as quasi-Newton method can be substituted.

4. EXPERIMENTS AND RESULTS

4.1. Compared with state-of-the-art techniques

We compare with other state-of-the-art approaches including GCV [29], APEX [23], kurtosis [21], DL1C [26] and bluSURE [19]. The blur size of Gaussian kernel is estimated and then compared with the ground truth parameter s_0. Table 1 reports the estimation results we have obtained for two standard test images (*Cameraman* and *Lake*), over two representative noise levels ($\alpha = 1, 10$) and two different ground truth blur sizes ($s_0 = 1.5, 3.0$). Fig. 3 shows typical examples of the blur-PURE minimization and the estimated $s \approx s_0$. It can be seen that the proposed approach generally yields more accurate and consistent estimation of the blur size s than other

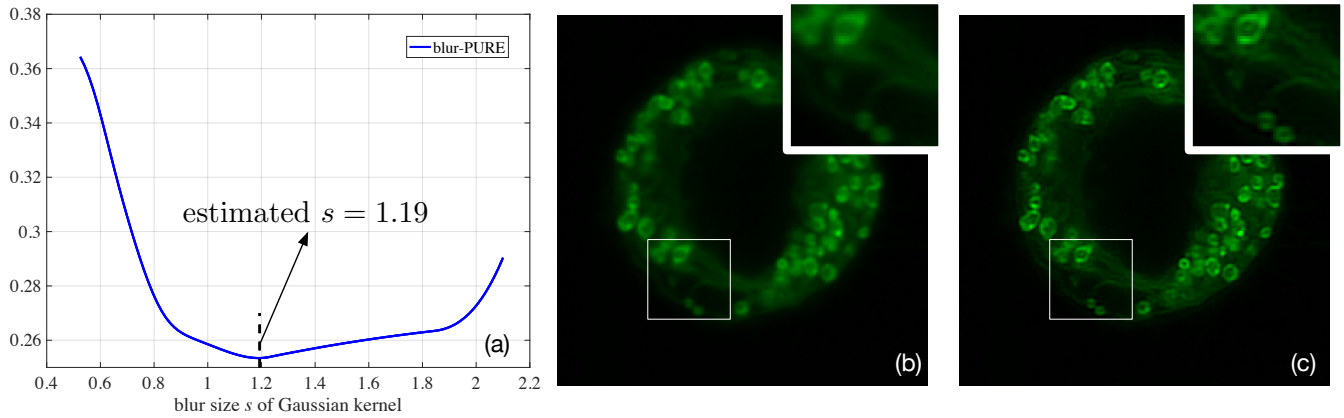

Fig. 4. Restoration of real fluorescence microscopy image. The blur parameter s is firstly estimated by the proposed blur-PURE approach (a), and the non-blind deconvolution algorithm in [9] is then applied on the measured image (b) to obtain the restored image (c). Fine structures of the cell can be seen.

Table 1. Comparison with state-of-the-art techniques for the estimation. Best estimation results are highlighted.

Image	*Cameraman*				*Lake*			
true s_0	$s_0 = 1.5$		$s_0 = 3.0$		$s_0 = 1.5$		$s_0 = 3.0$	
noise level α	1	10	1	10	1	10	1	10
GCV	1.80	2.24	3.72	3.23	1.81	2.05	3.53	3.04
APEX	1.36	1.12	1.62	1.28	0.78	0.78	1.61	0.93
kurtosis	1.55	1.83	2.92	2.35	2.05	2.25	3.29	3.56
DL1C	2.10	2.25	3.47	4.43	2.23	1.98	4.12	2.75
blur-SURE	1.75	2.78	3.43	3.01	1.91	2.11	3.51	3.79
blur-PURE	**1.49**	**1.52**	**2.98**	**3.02**	**1.53**	**1.57**	**3.05**	**3.02**

approaches. We would like to stress that the blur-PURE approach is very robust to high noise level. The computation time of the blur-PURE is similar to the blur-SURE [19] (less than 0.7 second for a 256×256 image), and thus also substantially faster than others (more than 1.2 seconds). All experiments are carried out on a Macbook Pro with a 2.8 GHz Intel Core i7, with 16 GB of RAM.

4.2. Blind deconvolution for fluorescence microscopy

We applied the proposed approach on a real fluorescence microscopy image of mitotic HeLa cell[2]. This 3D image is collected on a Leica TCS SP5 confocal laser scanning microscope with 63x/1.4 oil objective lens. We use one slice for illustration, which is of size 256×256. The pixel size is 120nm. As demonstrated in [15], the PSF in 2D confocal microscopy can be well approximated by a Gaussian kernel. The noise level is estimated as $\alpha = 0.02$ by the mentioned robust linear regression mechanism, and the blur size of the Gaussian kernel is estimated as $s = 1.19$ by the proposed approach. Then the non-blind deconvolution algorithm in [9] is applied. Fig. 4 shows the measured and restored images. It can be seen that the membranes have become more recognizable with respect to the background. Also, the filament structure is visible with significantly better contrast.

[2]http://www.cellimagelibrary.org/images/35158.

5. CONCLUSION

We proposed a parametric blur estimation method for photon-limited images. It is based on the blur-PURE, which is a statistical estimate of the *blur-MSE*. In conjunction with Wiener filtering, the blur-PURE minimization yields highly accurate blur estimation. Results obtained show that the proposed approach outperforms state-of-the-art techniques. Combined with our non-blind deconvolution algorithm [9], a high-quality blind deconvolution algorithm for photon-limited images can be obtained. Note that the blur-PURE minimization itself is not restricted to PSF that has a particular parametric form, even though we limited ourselves to Gaussian blur in this work.

6. REFERENCES

[1] P. Sarder and A. Nehorai, "Deconvolution methods for 3-D fluorescence microscopy images," *IEEE Signal Process. Mag.*, vol. 23, no. 3, pp. 32–45, 2006.

[2] M. Bertero, P. Boccacci, G. Desiderà, and G. Vicidomini, "Image deblurring with Poisson data: from cells to galaxies," *Inverse Probl.*, vol. 25, no. 12, pp. 123 006–27, 2009.

[3] M. Hirsch, S. Harmeling, S. Sra, and B. Schölkopf, "Online multi-frame blind deconvolution with super-resolution and saturation correction," *Astron. Astrophys*, vol. 531, p. A9, 2011.

[4] D. Sage, L. Donati, F. Soulez, D. Fortun, G. Schmit, A. Seitz, R. Guiet, C. Vonesch, and M. Unser, "Deconvolutionlab2: An open-source software for deconvolution microscopy," *Methods*, vol. 115, pp. 28–41, 2017.

[5] Z. T. Harmany, R. F. Marcia, and R. M. Willett, "This is SPIRAL-TAP: Sparse Poisson intensity reconstruction algorithms: theory and practice," *IEEE Trans. Image Process.*, vol. 21, no. 3, pp. 1084–1096, 2012.

[6] M. Carlavan and L. Blanc-Feraud, "Sparse Poisson noisy image deblurring," *IEEE Trans. Image Process.*, vol. 21, no. 4, pp. 1834–1846, 2012.

[7] S. Lefkimmiatis and M. Unser, "Poisson image reconstruction with Hessian Schatten-Norm regularization," *IEEE Trans. Image Process.*, vol. 22, no. 11, pp. 4314–4327, 2013.

[8] E. Chouzenoux, A. Jezierska, J.-C. Pesquet, and H. Talbot, "A convex approach for image restoration with exact Poisson-Gaussian likelihood." *SIAM J. Imaging Sci.*, vol. 8, no. 4, pp. 2662–2682, 2015.

[9] J. Li, F. Luisier, and T. Blu, "Deconvolution of Poissonian images with the PURE-LET approach," in *Proc. IEEE Int. Conf. Img. Proc. (ICIP)*, Phoenix, USA, 2016, pp. 2708–2712.

[10] S. Bonettini, R. Zanella, and L. Zanni, "A scaled gradient projection method for constrained image deblurring," *Inverse Probl.*, vol. 25, no. 1, p. 015002, 2008.

[11] M. Keuper, T. Schmidt, M. Temerinac-Ott, J. Padeken, P. Heun, O. Ronneberger, and T. Brox, "Blind deconvolution of wide-field fluorescence microscopic data by regularization of the optical transfer function (OTF)," in *Proc. IEEE Comput. Soc. Conf. Comput. Vis. Pattern Recognit. (CVPR)*, 2013, pp. 2179–2186.

[12] F. Soulez, "A "learn 2D, apply 3D" method for 3D deconvolution microscopy," in *Proc. IEEE Int. Symp. Biomed. Imaging (ISBI)*, Beijing, China, 2014, pp. 1075–1078.

[13] B. Kim and T. Naemura, "Blind depth-variant deconvolution of 3D data in wide-field fluorescence microscopy," *Sci. Rep.*, vol. 5, no. 9894, pp. 1–9, 2015.

[14] J. Li, F. Luisier, and T. Blu, "PURE-LET deconvolution of 3D fluorescence microscopy images," in *Proc. IEEE Int. Symp. Biomed. Imaging (ISBI)*, 2017, pp. 723–727.

[15] B. Zhang, J. Zerubia, and J.-C. Olivo-Marin, "Gaussian approximations of fluorescence microscope point-spread function models," *Appl. Opt.*, vol. 46, no. 10, pp. 1819–1829, 2007.

[16] P. Pankajakshan, B. Zhang, L. Blanc-Féraud, Z. Kam, J.-C. Olivo-Marin, and J. Zerubia, "Blind deconvolution for thin-layered confocal imaging," *Appl. Opt.*, vol. 48, no. 22, pp. 4437–4448, 2009.

[17] J. Markham and J.-A. Conchello, "Parametric blind deconvolution: a robust method for the simultaneous estimation of image and blur," *J. Opt. Soc. Am. A*, vol. 16, no. 10, pp. 2377–2391, 1999.

[18] T. Kenig, Z. Kam, and A. Feuer, "Blind image deconvolution using machine learning for three-dimensional microscopy," *IEEE Trans. Pattern Anal. Mach. Intell.*, vol. 32, no. 12, pp. 2191–2204, Dec. 2010.

[19] F. Xue and T. Blu, "A novel SURE-based criterion for parametric PSF estimation," *IEEE Trans. Image Process.*, vol. 24, no. 2, pp. 595–607, 2015.

[20] J. P. Oliveira, M. A. Figueiredo, and J. M. Bioucas-Dias, "Parametric blur estimation for blind restoration of natural images: Linear motion and out-of-focus," *IEEE Trans. Image Process.*, vol. 23, no. 1, pp. 466–477, 2014.

[21] D. Li, R. M. Mersereau, and S. Simske, "Atmospheric turbulence-degraded image restoration using principal components analysis," *IEEE Geosci. Remote Sens. Lett.*, vol. 4, no. 3, pp. 340–344, 2007.

[22] A. S. Carasso, "APEX blind deconvolution of color hubble space telescope imagery and other astronomical data," *Opt. Eng.*, vol. 45, no. 10, pp. 107 004–107 004, 2006.

[23] ——, "The APEX method in image sharpening and the use of low exponent lévy stable laws," *SIAM J. Appl. Math.*, vol. 63, no. 2, pp. 593–618, 2002.

[24] F. Soulez, L. Denis, Y. Tourneur, and É. Thiébaut, "Blind deconvolution of 3D data in wide field fluorescence microscopy," in *Proc. IEEE Int. Symp. Biomed. Imaging (ISBI)*. IEEE, 2012, pp. 1735–1738.

[25] L. Chen and K.-H. Yap, "A soft double regularization approach to parametric blind image deconvolution," *IEEE Trans. Image Process.*, vol. 14, no. 5, pp. 624–633, 2005.

[26] F. Chen and J. Ma, "An empirical identification method of Gaussian blur parameter for image deblurring," *IEEE Trans. Signal Process.*, vol. 57, no. 7, pp. 2467–2478, 2009.

[27] Q. Cao, "Generalized jinc functions and their application to focusing and diffraction of circular apertures," *J. Opt. Soc. Am. A*, vol. 20, no. 4, pp. 661–667, 2003.

[28] G. Urcid and A. Padilla, "Far-field diffraction patterns of circular sectors and related apertures," *Appl. Opt.*, vol. 44, no. 36, pp. 7677–7696, 2005.

[29] S. J. Reeves and R. M. Mersereau, "Blur identification by the method of generalized cross-validation," *IEEE Trans. Image Process.*, vol. 1, no. 3, pp. 301–311, 1992.

[30] F. Luisier, T. Blu, and M. Unser, "Image denoising in mixed Poisson-Gaussian noise," *IEEE Trans. Image Process.*, vol. 20, no. 3, pp. 696–708, 2011.

[31] J. Boulanger, C. Kervrann, P. Bouthemy, P. Elbau, J.-B. Sibarita, and J. Salamero, "Patch-based nonlocal functional for denoising fluorescence microscopy image sequences," *IEEE Trans. Med. Imag.*, vol. 29, no. 2, pp. 442–454, 2010.